OUKA
The University of Osaka
Institutional Knowledge Archive

Title	Post-Translational Isoaspartate Promotes Amyloid Formation in β_2-Microglobulin
Author(s)	Kawakami, Ryuji; Takei, Toshiki; So, Masatomo et al.
Citation	Angewandte Chemie - International Edition. 2026, 65(30), p. e7045464
Version Type	VoR
URL	https://hdl.handle.net/11094/105919
rights	This article is licensed under a Creative Commons Attribution-NonCommercial-NoDerivatives 4.0 International License.
Note	

The University of Osaka Institutional Knowledge Archive : OUKA

https://ir.library.osaka-u.ac.jp/

The University of Osaka

Check for updates

Angewandte Chemie International Edition

Angewandte International Edition Chemie

How to cite: *Angew. Chem. Int. Ed.* **2026**, e7045464
doi.org/10.1002/anie.7045464

COMMUNICATION OPEN ACCESS Hot Paper

Post-Translational Isoaspartate Promotes Amyloid Formation in β_2-Microglobulin

Ryuji Kawakami[1] | Toshiki Takei[1] | Masatomo So[2] | Toshifumi Takao[1,3] | Yoshinori Taguchi[1] | Hironobu Hojo[1]

[1]Institute for Protein Research, The University of Osaka, Suita, Osaka, Japan | [2]Graduate School of Agriculture, Kyoto University, Kyoto, Japan | [3]Rigaku Corporation, Akishima, Tokyo, Japan

Correspondence: Hironobu Hojo (hojo@protein.osaka-u.ac.jp)

Received: 14 February 2026 | **Revised:** 7 May 2026 | **Accepted:** 27 May 2026

Keywords: β_2-microglobulin | amyloid fibril formation | chemical synthesis | isoaspartate

ABSTRACT

β_2-Microglobulin (β2m) aggregation is central to dialysis-related amyloidosis (DRA), yet the molecular triggers underlying its fibrillogenesis remain incompletely defined. Among proposed mechanisms, isoaspartate (isoAsp) formation at Asn residues has been implicated but never directly tested due to synthetic inaccessibility. Here, we report the total chemical synthesis of β2m variants containing isoAsp at known in vivo hotspots, Asn^{17} and Asn^{42}, enabling precise structural and functional interrogation. Remarkably, the isoAsp^{17}-modified β2m exhibited greater fibril formation capacity than the pathogenic ΔN6-β2m variant, suggesting a previously underappreciated contribution of isoAsp^{17}. Structural characterization was complemented by spectroscopic and TEM analyses, which demonstrated that isoAsp^{17} promotes fibril formation. Our findings provide the first direct experimental evidence that a spontaneous post-translational modification can initiate amyloidogenesis in β2m, redefining the molecular basis of DRA and highlighting isoAsp as a general driver of pathological protein aggregation.

β_2-Microglobulin (β2m) is a component of major histocompatibility complex class I (MHC-I) molecules, which are expressed on the surface of all nucleated cells and function in the presentation of endogenous antigens to cytotoxic T cells [1]. During MHC-I turnover, β2m is released into circulation and normally cleared by the kidneys. In healthy individuals, its serum concentration remains around 1–2 mg/L. However, in patients with impaired renal function undergoing long-term dialysis, β2m cannot be efficiently removed, even with advanced dialysis membranes, and accumulates to levels exceeding 40 mg/L [2]. Prolonged β2m accumulation leads to the formation of amyloid fibrils, particularly in joint tissues, causing dialysis-related amyloidosis (DRA)—a debilitating condition that significantly impairs patient mobility. Although β2m's involvement in DRA has been firmly established, the precise molecular mechanisms underlying its amyloidogenic transformation remain incompletely understood. One known pathological variant is ΔN6, a β2m isoform lacking the six N-terminal residues, which has been consistently identified in amyloid deposits from DRA patients [3–6]. ΔN6 exhibits reduced structural stability and enhanced fibril formation compared to the native protein, providing key insights into how structural alterations can promote β2m misfolding.

In addition to such proteolytic variants, previous studies have highlighted the role of spontaneous post-translational modifications, particularly non-enzymatic deamidation of asparagine (Asn) residues [7, 8]. β2m contains two Asn-Gly sequences—Asn^{17}-Gly^{18} and Asn^{42}-Gly^{43}—which are known hotspots for deamidation [9]. This non-enzymatic process is a ubiquitous molecular aging reaction that affects long-lived proteins and has

Ryuji Kawakami and Toshiki Takei contributed equally to this work.

This is an open access article under the terms of the Creative Commons Attribution-NonCommercial-NoDerivs License, which permits use and distribution in any medium, provided the original work is properly cited, the use is non-commercial and no modifications or adaptations are made.
© 2026 The Author(s). *Angewandte Chemie International* Edition published by Wiley-VCH GmbH

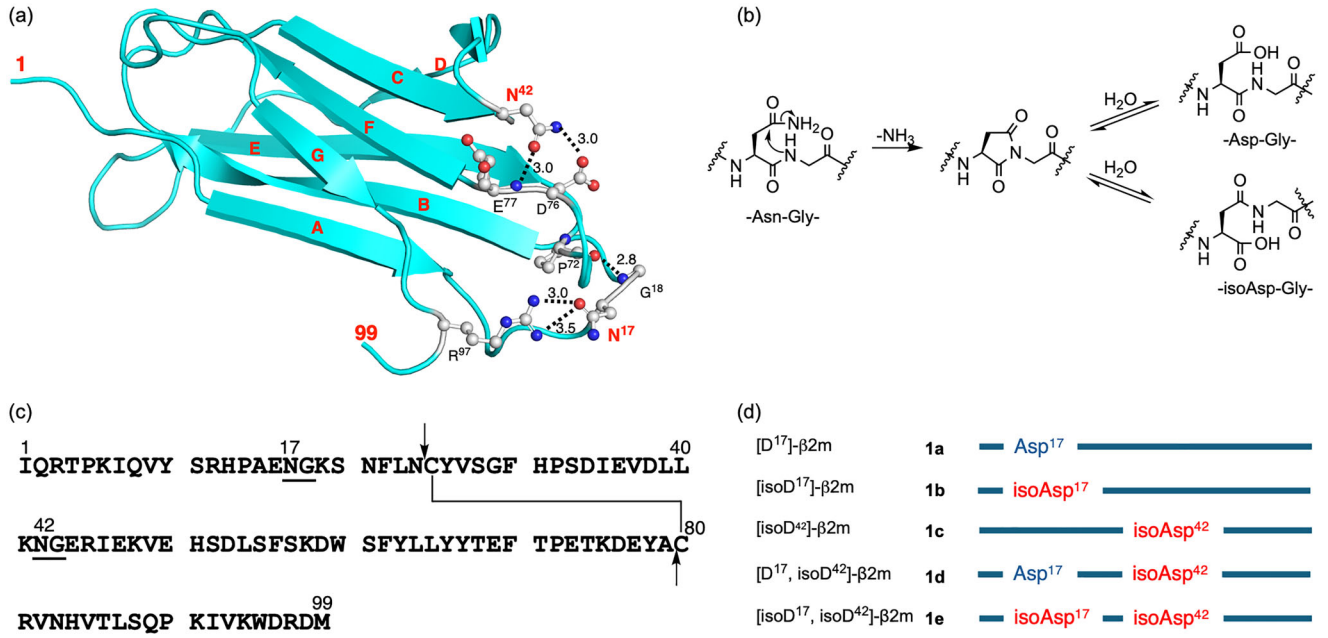


FIGURE 1 | (a) Structural basis for the differential impact of Asn[17] and Asn[42] isomerization on β2m stability. Asn[17] forms a hydrogen bond network with Arg[97], connecting the N-terminal AB loop and the C-terminal FG loop. In contrast, Asn[42] interacts locally with Asp[76] and Glu[77] within the same β-sheet (PDB: 2axf, resolution: 1.80 Å). (b) The mechanism of deamidation at the -Asn-Gly- sequence, (c) amino acid sequence of β2m. The arrows indicate the site of ligation. (d) Synthesized β2m variants.

been implicated in various pathological conditions, including neurodegenerative diseases and systemic amyloidoses. Deamidation converts Asn into either aspartate (Asp) or isoaspartate (isoAsp), with the latter introducing a β-peptide linkage that shifts the protein backbone and potentially destabilizes the structure (Figure 1b). Our previous analysis showed that Asn[17] undergoes deamidation more readily than Asn[42], with a nearly equal distribution of Asp and isoAsp products (Asn:Asp:isoAsp = 28:40:32), whereas Asn[42] predominantly forms isoAsp (Asn:Asp:isoAsp = 89:0.4:10.6) [10].

Although recombinant expression systems have facilitated analysis of Asp substitutions [11], the incorporation of isoAsp cannot be achieved by these methods. In contrast, recent advances in the chemical synthesis of proteins have enabled the preparation of native and post-translationally modified proteins for structural and functional studies [12, 13]. Building on these advances, in this study, we aimed to elucidate the impact of site-specific deamidation by chemically synthesizing β2m variants containing Asp or isoAsp at Asn[17] and/or Asn[42] (Figure 1d). Through comparative biophysical analyses with the ΔN6 variant, we demonstrate that the isoAsp[17] modification markedly destabilizes β2m and accelerates fibril formation under physiological conditions. These findings provide direct evidence that isoAsp formation at Asn[17] serves as a potent molecular trigger of β2m amyloidogenesis and may represent a novel therapeutic target in DRA.

β2m is a 99-residue protein that contains a single disulfide bond. The amino acid sequence is shown in Figure 1c. In this study, we planned to synthesize the full-length sequence using the native chemical ligation (NCL) method [14] with two cysteine residues forming the disulfide bond serving as the condensation sites. The entire sequence was divided into three segments: N-terminal (1–24), middle (25–79), and C-terminal (80–99). To realize the synthesis of the β2m variants, **1a**–**1e**, we prepared the N-terminal with Asp[17] **2a**, isoAsp[17] **2b**, and Asn[17] **2c**, middle with isoAsp[42] **3a** and Asn[42] **3b**, and C-terminal segment **4** (Figure S1) by the solid-phase method [15]. The NCL reaction was then performed. When synthesizing peptides containing an Asp-Gly sequence using the prevalent 9-fluorenylmethoxycarbonyl (Fmoc) strategy, it is known that the aspartimide formation during piperidine treatment usually occurs as a major side reaction. To suppress this, a dipeptide unit with the 2,4-dimethoxybenzylated amide between Asp and Gly is frequently used [16]. On the other hand, in the *t*-butoxycarbonyl (Boc) strategy, it is known that aspartimide formation can be suppressed by using a cyclohexyl (cHex) ester for Asp side chain protection [17]. In addition, the peptide thioester, essential for the ligation of the peptides by the NCL, can be directly synthesized by the Boc method. Therefore, the N-terminal and middle segments, which retain the Asp-Gly or isoAsp-Gly sequence, were synthesized by the Boc strategy using the in situ neutralization method [18].

As an example, the synthesis of the N-terminal segment with isoAsp[17] **2b** is shown in Figure S5. To the p-methylbenzhydrylamine (MBHA) resin, Boc-Ala-OH was introduced by the O-(1H-benzotriazol-1-yl)-N,N,N′,N′-tetramethyluronium hexafluorophosphate (HBTU)/N,N-diisopropylethylamine (DIEA) method. This residue is essential to avoid the cleavage of the peptide chain from the resin during the Boc group removal by trifluoroacetic acid (TFA) treatment [19]. S-Triphenylmethyl (Trt)-protected 3-mercaptopropionic acid (MPA) was introduced by the same procedure. After removal of the Trt group by TFA containing triethylsilane (TES), the thioester linkage was formed by introducing the C-terminal amino acid by HBTU and DIEA. The remaining peptide chain

15213773, 0, Downloaded from https://onlinelibrary.wiley.com/doi/10.1002/anie.7045464 by The University Of Osaka, Wiley Online Library on [15/06/2026]. See the Terms and Conditions (https://onlinelibrary.wiley.com/terms-and-conditions) on Wiley Online Library for rules of use; OA articles are governed by the applicable Creative Commons License

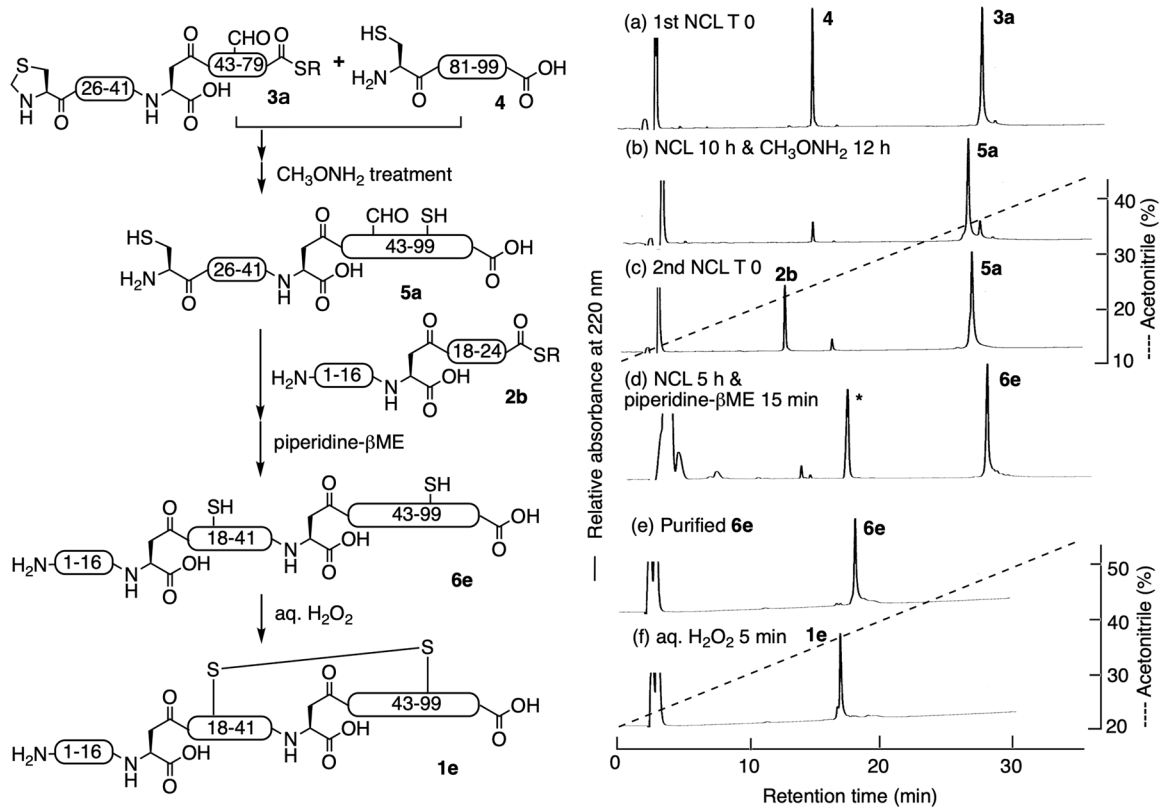


FIGURE 2 | Synthetic route of β2m variant **1e**. *: Non-peptide.

was elongated by the Boc method. For the introduction of the 17th amino acid residue, Boc-Asp-OcHex, which has the free side chain carboxy group, was introduced to form the isoAsp bond. After the complete assembly of the peptide chain, the protected peptide resin was treated with HF containing anisole as a cation scavenger to obtain the crude peptide thioester, which underwent reversed-phase high-performance liquid chromatography (RPHPLC) to obtain the purified peptide **2b**. The other N-terminal and middle segments were synthesized in a similar manner by the Boc method (See Supporting Information). The C-terminal segment **4** was prepared by the Fmoc method (Figure S9).

Having all the segments in hand, the ligation of the segments by the NCL method was performed as exemplified in the case of variant **1e** in Figure 2. The middle **3a** and the C-terminal segment **4** were dissolved in a phosphate buffer (pH 7.0) containing 4-mercaptophenylacetic acid (MPAA), tris(2-carboxyethyl)phosphine (TCEP) hydrochloride, and guanidinium hydrochloride (GuHCl), and the condensation reaction was carried out by stirring under an argon atmosphere at room temperature in the dark. The reaction was completed in approximately 10 h, and the desired product was obtained as the main product. Subsequently, aq. CH_3ONH_2·HCl was added, and the pH was adjusted to 4.0 using aq. HCl to open the N-terminal thiazolidine ring. After 12 h, the reaction was completed to obtain peptide **5a**, which was monitored by RPHPLC and electrospray ionization (ESI)-mass spectrometry (MS). The product was purified by RPHPLC to obtain the desired product **5a** in 47% yield based on peptide **3a**. The ligation of the N-terminal segment **2b** and intermediate **5a** was also performed in a similar manner, and the entire polypeptide of β2m was assembled. A mixed solution of piperidine and 2-mercaptoethanol (βME) was then added and stirred to remove the formyl group on the Trp side chain. After 15 min, the product was purified by RPHPLC to obtain peptide **6e** in 67% yield based on peptide **5a**. The obtained peptide **6e** was dissolved in a phosphate buffer (pH 7.1) containing GuHCl, and aq. hydrogen peroxide was added to form the SS bond. After 5 min, the reaction was completed, and the product was isolated by RPHPLC to obtain **1e** in 59% yield based on peptide **6e**. The other β2m variants, **1a** to **1d**, were also synthesized in a similar manner.

To verify that the chemically synthesized β2m variants retained their native-like structures, circular dichroism (CD) spectra were measured under physiological buffer conditions (20 mM phosphate, pH 7.0). All variants, including the wild-type, exhibited a characteristic negative peak around 220 nm and a positive peak near 202 nm (Figure 3a), consistent with the typical immunoglobulin fold of β2m. Notably, the isoAsp[17]-containing variants, **1b** and **1e**, showed a marked reduction in both peaks, suggesting an increase in random coil content and a disruption of the native secondary structure. In contrast, the isoAsp[42] variants, **1c** and **1d**, exhibited only a slight attenuation of the spectral features compared to the wild-type, indicating relatively minor structural alterations. These results imply that isomerization at Asn[17] has a more pronounced destabilizing effect on β2m structure than at Asn[42]. Our structural interpretation is further supported by the crystal structure of β2m (PDB: 2axf, 1.80 Å resolution), which clearly visualizes a hydrogen bond network between the side chain of Asn[17] and the guanidinium group of Arg[97] (Figure 1a). This interaction connects the N-terminal AB loop with the C-terminal FG loop, suggesting that Asn[17] plays a role in stabilizing

15213773, 0, Downloaded from https://onlinelibrary.wiley.com/doi/10.1002/anie.7045464 by The University Of Osaka, Wiley Online Library on [15/06/2026]. See the Terms and Conditions (https://onlinelibrary.wiley.com/terms-and-conditions) on Wiley Online Library for rules of use; OA articles are governed by the applicable Creative Commons License

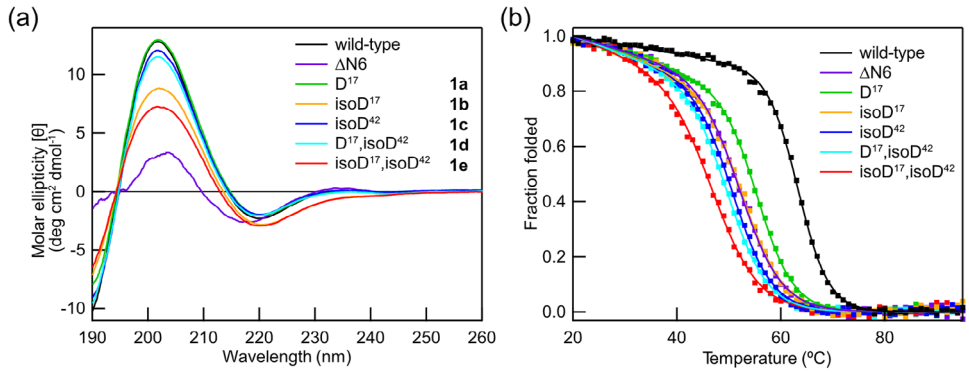


FIGURE 3 | (a) Secondary structure of wild-type and variant β2m confirmed by CD spectra. (b) Temperature dependence of CD intensities monitored at 205 nm (dots). The lines represent the fitting curves analyzed by the two-state denaturation model. Data were normalized using fitting values. The physicochemical parameters obtained are shown in Table 1.

TABLE 1 | Physicochemical parameters of heat denaturation of β2ms.

	T_m (°C)[a]	ΔH_U (×10^5 J/mol)[a]	ΔS_U (J/mol K)[a]	ΔG_U (×10^5 J/mol)[a]
WT	63.6 ± 0.05	3.03 ± 0.17	901 ± 49	1.67 ± 1.23
ΔN6	52.8 ± 0.15	2.20 ± 0.07	674 ± 22	1.26 ± 1.00
D^{17} **1a**	55.8 ± 0.12	2.35 ± 0.24	715 ± 72	1.28 ± 0.98
isoD^{17} **1b**	53.3 ± 0.14	2.24 ± 0.10	685 ± 31	1.28 ± 1.01
isoD^{42} **1c**	51.5 ± 0.20	2.40 ± 0.08	740 ± 25	1.40 ± 1.13
D^{17}, isoD^{42} **1d**	50.6 ± 0.27	2.45 ± 0.18	757 ± 54	1.46 ± 1.19
isoD^{17}, isoD^{42} **1e**	47.8 ± 0.33	1.99 ± 0.03	619 ± 10	1.16 ± 0.95

[a]T_m, ΔH_U, ΔS_U, and ΔG_U represent the transition midpoint, and the enthalpy, entropy, and Gibbs free energy of unfolding, respectively. Errors represent standard deviations (SD) from 3 independent experiments.

the global β-sandwich architecture through long-range interloop interactions. Isomerization of Asn^{17} to isoAsp is likely to disrupt this specific interaction, contributing to conformational destabilization.

In contrast, Asn^{42} is located in the CD loop and forms hydrogen bonds with residues Asp^{76} and Glu^{77}, which are part of the loop connecting the E and F strands. While these interactions help stabilize the adjacent β-sheet region, they are spatially more localized and may have a more limited effect on the global β-sandwich conformation. Compared to the long-range interaction between Asn^{17} and Arg^{97}, the structural impact of isomerization at Asn^{42} is likely to be more limited, which aligns with the relatively minor changes observed in the CD spectra of isoAsp^{42}-containing variants. The greater susceptibility of Asn^{17} to deamidation under physiological conditions [10] further supports its structural lability and functional relevance, whereas isoAsp^{42} formation may be a less common and less disruptive event in vivo.

The stability of the structure of the β2m variants was analyzed by the change in the CD spectrum upon heating. Wild-type- and ΔN6-β2m [3–6] stability was also assessed for comparison. All the β2m variants showed a decreased stability compared to the WT (Figure 3b and Table 1). The ΔN6-, isoAsp^{17}- and isoAsp^{42}-β2m variants, **1b**-**1d**, showed a comparable thermal stability, while isoAsp^{17,42}-β2m **1e** showed a further decreased stability, indicating that the Asn to isoAsp conversion significantly decreased the stability of β2m.

To assess whether mutations at Asn^{17} or Asn^{42} promote amyloidogenesis by destabilizing the native β2m structure, we evaluated the fibril-forming abilities of synthetic β2m variants using thioflavin T (ThT) fluorescence assays. Samples were prepared in phosphate buffer (pH 6.2) containing 115 mM NaCl and 5 μM ThT, with a final β2m concentration of 25 μM. The mixtures were incubated at 37°C with agitation, and fluorescence intensity was monitored at 485 nm (excitation at 445 nm). Figure S22 shows the normalized ThT fluorescence profiles. Variants **1b** and **1e**, both containing isoAsp^{17}, exhibited accelerated fibril formation. Their half-times ($T_{1/2}$) to reach 50% of maximum fluorescence are shown in Figure 4a. These isoAsp^{17} variants aggregated more rapidly than the ΔN6 variant, which is itself known for rapid fibril formation. Transmission electron microscopy (TEM) images (Figure 4b) confirmed the presence of long, unbranched fibrils in the samples containing variants **1b**, **1e**, and ΔN6. In contrast, variants **1c** and **1d**, which carry isoAsp^{42}, showed no significant increase in ThT fluorescence (Figure 4a), suggesting a lack of typical amyloid fibril formation. However, TEM analysis revealed that these variants exhibited abnormal behavior compared to the wild-type, forming amorphous or irregular aggregates rather than remaining as soluble monomers. This observation suggests that while the isoAsp^{42} modification destabilizes the native fold

15213773, 0, Downloaded from https://onlinelibrary.wiley.com/doi/10.1002/anie.70454 64 by The University Of Osaka, Wiley Online Library on [15/06/2026]. See the Terms and Conditions (https://onlinelibrary.wiley.com/terms-and-conditions) on Wiley Online Library for rules of use; OA articles are governed by the applicable Creative Commons License

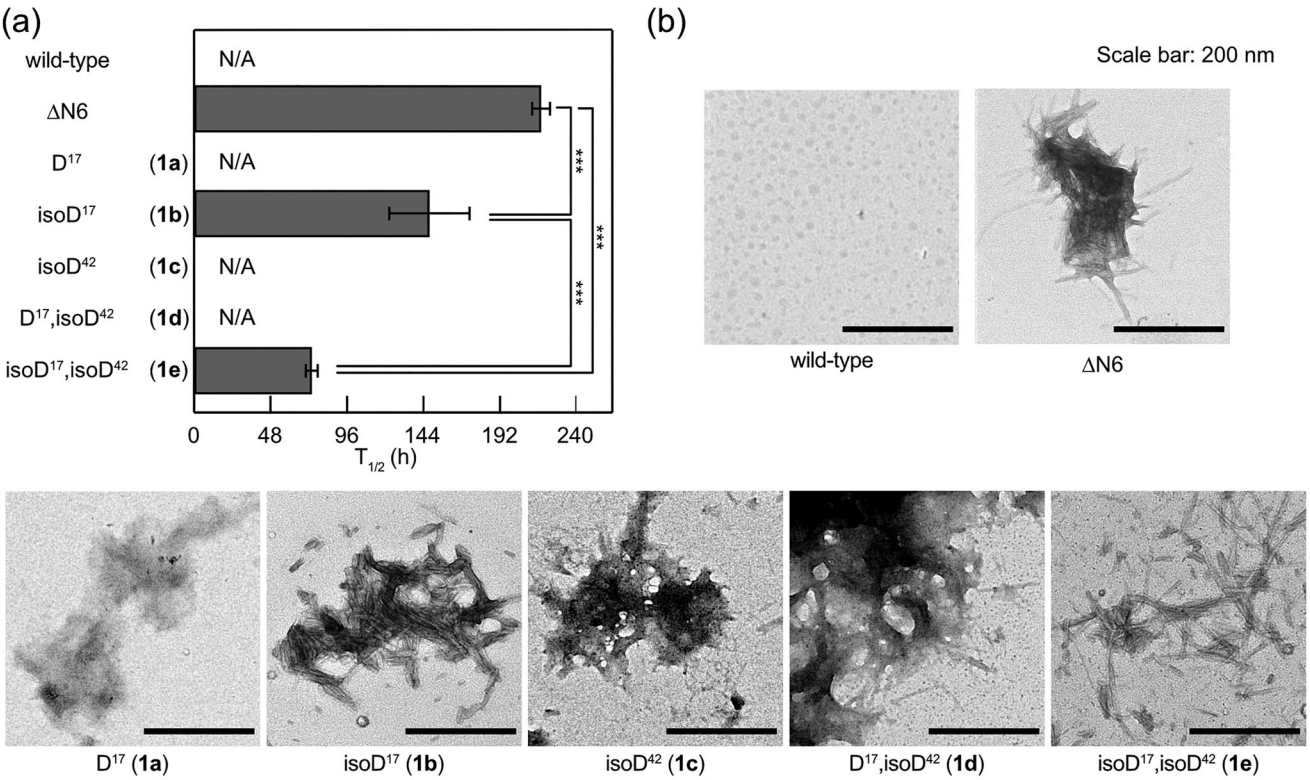


FIGURE 4 | Amyloid formation of β2m variants. (a) The $T_{1/2}$ values were calculated using ThT kinetics (Figure S22) for ΔN6-, isoAsp^{17}-, and isoAsp^{17}, isoAsp^{42}-β2m, which showed a significant increase in ThT. N/A represents no significant increase in ThT. Error bars represent the standard deviation (SD) of four (for [isoAsp^{17}, isoAsp^{42}]-β2m) or five (for others) independent replicates. Statistical significance was determined by one-way ANOVA followed by the Tukey–Kramer post-hoc test. ***$p < 0.001$. (b) TEM images of the fibrils formed by the β2m variants. Scale bars represent 200 nm.

to some extent, it simultaneously reduces the amyloidogenic potential of the protein, instead promoting the formation of ThT-negative amorphous species due to the overall decrease in structural stability.

The 3D structure of the ΔN6-derived fibril (PDB: 8a7o) revealed that both Asn^{17} and Asn^{42} are located near inter- or intra-molecular interfaces within the oligomeric assembly (Figure S23), suggesting that isomerization from Asn to isoAsp at these positions substantially alters the molecular architecture to favor fibril formation. The distinct fibril morphologies between **1b**/**1e**/ΔN6 and **1c**/**1d** may be attributed to differences in the structural roles of Asn^{17} and Asn^{42}. While both residues are located near inter- or intra-molecular interfaces (Figure S23), Asn^{42} resides near a flexible β-turn region, potentially modulating protofilament packing and lateral assembly. In contrast, Asn^{17} is situated at a more rigid interface crucial for stabilizing the fibrillar core.

In this context, it is noteworthy that another localized conformational change—the cis–trans isomerization of the Pro^{32} peptide bond, located structurally between positions 17 and 42—has also been identified as a trigger for β2m aggregation. Previous work by Torbeev and Hilvert demonstrated that a synthetic β2m analog locked in the trans-Pro^{32} conformation promotes the exposure of hydrophobic patches and drives amorphous aggregation, similar to the behavior we observed for our isoAsp^{42}-containing variants (**1c**/**1d**) [20]. However, because the trans-Pro^{32} analog alone did not form typical amyloid fibrils, they proposed that a partial or transient cis-to-trans conversion may act synergistically to initiate oligomerization and subsequent fibril formation. Thus, while Pro^{32} isomerization is a distinct event, the respective roles of Pro^{32} conformational dynamics and isoAsp-induced destabilization—particularly the potent amyloidogenic effect we observed for isoAsp^{17}—likely represent independent yet complementary factors within the complex β2m fibrillization pathway.

Therefore, isomerization at Asn^{17} likely disrupts the core architecture more directly than Asn^{42}, leading to enhanced amyloidogenicity and more uniform fibril formation. Furthermore, fibrils derived from isoAsp^{17}-containing variants effectively acted as seeds to promote fibrillization of wild-type β2m monomer (Figure S24), highlighting their nucleating potential. Taken together and considering the longer in vivo half-life of Asn^{42} deamidation relative to Asn^{17} [10], our results indicate that isoAsp formation at Asn^{17} is likely a more critical driver of β2m amyloidogenesis.

In conclusion, this study demonstrates that site-specific deamidation at the Asn-Gly site, particularly the formation of isoAsp at position 17, markedly destabilizes β2m and enhances its propensity for amyloid fibril formation. The aggregation rate of the isoAsp^{17} variant exceeds that of the ΔN6 variant and facilitates fibril seeding of the wild-type protein. These findings implicate isoAsp formation at Asn^{17} as a critical early event in DRA pathogenesis. Moreover, this work highlights the utility

15213773, 0, Downloaded from https://onlinelibrary.wiley.com/doi/10.1002/anie.7045464 by The University Of Osaka, Wiley Online Library on [15/06/2026]. See the Terms and Conditions (https://onlinelibrary.wiley.com/terms-and-conditions) on Wiley Online Library for rules of use; OA articles are governed by the applicable Creative Commons License

of chemical synthesis in precisely modeling post-translational modifications, offering valuable tools for understanding amyloid mechanisms and exploring therapeutic strategies.

Author Contributions

Ryuji Kawakami: investigation. **Toshiki Takei:** data curation, supervision, investigation. **Masatomo So:** investigation, data curation. **Toshifumi Takao:** conceptualization, data curation, writing – review and editing. **Yoshinori Taguchi:** investigation. **Hironobu Hojo:** writing – review and editing, writing – original draft, project administration, data curation, supervision, investigation.

Acknowledgments

This work was supported in part by KAKENHI grants from the Ministry of Education, Culture, Sports, Science and Technology (MEXT)/Japan Society for the Promotion of Science (JSPS) (JP24K17788 for T. Takei, JP25K00268 for M.S. and JP23K23464 for H.H.), This work was performed in part under the Collaborative Research Program of Institute for Protein Research, The University of Osaka, CR-24-02. This work was also supported by ISHIZUE 2024 of Kyoto University. Part of the TEM observation was supported by the North Campus Instrumental Analysis Station, Kyoto University.

Conflicts of Interest

The authors declare no conflicts of interest.

Data Availability Statement

The data that support the findings of this study are available from the corresponding author upon reasonable request.

References

1. L. Strominger, D. C. Wiley, P. J. Bjorkman, M. A. Saper, B. Samraoui, and W. S. Bennett, "HLA-A2," *Nature* 329 (1987): 506–512.

2. J. Floege, A. Bartssch, M. Schulze, S. Shaldon, K. Koch, and L. Smeby, "Clearance and Synthesis Rates of Beta 2-Microglobulin in Patients Undergoing Hemodialysis and in Normal Subjects," *Journal of Laboratory and Clinical Medicine* 118 (1991): 153–165.

3. R. P. Linke, H. Hampl, H. Lobeck, et al., "Lysine-Specific Cleavage of β2-Microglobulin in Amyloid Deposits Associated with Hemodialysis," *Kidney International* 36 (1989): 675–681, https://doi.org/10.1038/ki.1989.245.

4. M. Stoppini, P. Arcidiaco, P. Mangione, S. Giorgetti, D. Brancaccio, and V. Bellotti, "Detection of Fragments of β2-Microglobulin in Amyloid Fibrils," *Kidney International* 57 (2000): 349–350, https://doi.org/10.1046/j.1523-1755.2000.00851.x.

5. G. Esposito, R. Michelutti, G. Verdone, et al., "Removal of the N-Terminal Hexapeptide from Human β2-Microglobulin Facilitates Protein Aggregation and Fibril Formation," *Protein Science* 9 (2000): 831–845, https://doi.org/10.1110/ps.9.5.831.

6. S. L. Myers, S. Jones, T. R. Jahn, et al., "A Systematic Study of the Effect of Physiological Factors on β2-Microglobulin Amyloid Formation at Neutral pH," *Biochemistry* 45 (2006): 2311–2321, https://doi.org/10.1021/bi052434i.

7. M. Stoppini, P. Mangione, M. Monti, et al., "Proteomics of β2-Microglobulin Amyloid Fibrils," *Biochim Biophys Acta Proteins Proteom* 1753 (2005): 23–33, https://doi.org/10.1016/j.bbapap.2005.07.019.

8. H. Odani, R. Oyama, K. Titani, H. Ogawa, and A. Saito, "Purification and Complete Amino Acid Sequence of Novel β2-Microglobulin," *Biochemical and Biophysical Research Communications* 168 (1990): 1223–1229, https://doi.org/10.1016/0006-291X(90)91159-P.

9. R. C. Stephenson and S. Clarke, "Succinimide Formation from Aspartyl and Asparaginyl Peptides as a Model for the Spontaneous Degradation of Proteins," *Journal of Biological Chemistry* 264 (1989): 6164–6170, https://doi.org/10.1016/S0021-9258(18)83327-0.

10. M. Fukuda and T. Takao, "Quantitative Analysis of Deamidation and Isomerization in β2-Microglobulin by 18O Labeling," *Analytical Chemistry* 84 (2012): 10388–10394, https://doi.org/10.1021/ac302603b.

11. N. M. Kad, N. H. Thomson, D. P. Smith, D. A. Smith, and S. E. Radford, "β2-microglobulin and Its Deamidated Variant, N17D form Amyloid Fibrils With a Range of Morphologies in Vitro," *Journal of Molecular Biology* 313 (2001): 559–571, https://doi.org/10.1006/jmbi.2001.5071.

12. V. Agouridas, O. E. Mahdi, and O. Melnyk, "Chemical Protein Synthesis in Medicinal Chemistry," *Journal of Medicinal Chemistry* 63 (2020): 15140–15152, https://doi.org/10.1021/acs.jmedchem.0c01082.

13. H. Ai, M. Pan, and L. Liu, "Chemical Synthesis of Human Proteoforms and Application in Biomedicine," *ACS Central Science* 10 (2024): 1442–1459, https://doi.org/10.1021/acscentsci.4c00642.

14. P. E. Dawson, T. W. Muir, I. Clark-Lewis, and S. B. H. Kent, "Synthesis of Proteins by Native Chemical Ligation," *Science* 266 (1994): 776–779, https://doi.org/10.1126/science.7973629.

15. R. B. Merrifield, "Solid Phase Peptide Synthesis. I. The Synthesis of a Tetrapeptide," *Journal of the American Chemical Society* 85 (1963): 2149–2154, https://doi.org/10.1021/ja00897a025.

16. V. Cardona, I. Eberle, S. Barthélémy, et al., "Application of Dmb-dipeptides in the Fmoc SPPS of Difficult and Aspartimide-Prone Sequences," *International Journal of Peptide Research and Therapeutics* 14 (2008): 285–292, https://doi.org/10.1007/s10989-008-9154-z.

17. J. P. Tam, T. W. Wong, M. W. Riemen, F. S. Tjoeng, and R. B. Merrifield, "Cyclohexyl Ester as a New Protecting Group for Aspartyl Peptides to Minimize Aspartimide Formation in Acidic and Basic Treatments," *Tetrahedron Letters* 20 (1979): 4033–4036, https://doi.org/10.1016/S0040-4039(01)86496-0.

18. M. Schnölzer, P. Alewood, A. Jones, D. Alewood, and S. B. H. Kent, "In Situ Neutralization in Boc-Chemistry Solid Phase Peptide Synthesis," *International Journal of Peptide and Protein Research* 40 (1992): 180–193, https://doi.org/10.1111/j.1399-3011.1992.tb00291.x.

19. H. Hojo, Y. Kwon, Y. Kakuta, et al., "Development of a Linker With an Enhanced Stability for the Preparation of Peptide Thioesters and Its Application to the Synthesis of a Stable-Isotope-Labelled HU-Type DNA-Binding Protein," *Bulletin of the Chemical Society of Japan* 66 (1993): 2700–2706, https://doi.org/10.1246/bcsj.66.2700.

20. V. Y. Torbeev and D. Hilvert, "Both the Cis-trans Equilibrium and Isomerization Dynamics of a Single Proline Amide Modulate β2-Microglobulin Amyloid Assembly," *Proceedings National Academy of Science USA* 110 (2013): 20051–20056, https://doi.org/10.1073/pnas.1310414110.

Supporting Information

Additional supporting information can be found online in the Supporting Information section.

Supporting File: anie73088-sup-0001-SuppMat.pdf.

15213773, 0, Downloaded from https://onlinelibrary.wiley.com/doi/10.1002/anie.7045464 by The University Of Osaka, Wiley Online Library on [15/06/2026]. See the Terms and Conditions (https://onlinelibrary.wiley.com/terms-and-conditions) on Wiley Online Library for rules of use; OA articles are governed by the applicable Creative Commons License